*Chinese J. Chem. Eng.*, **13** (2) 225 – 233 (2005)

# Low Temperature One-Step Synthesis of Barium Titanate: Thermodynamic Modeling and Experimental Synthesis*

**SHEN Zhigang(沈志刚), LI Shigang(李世刚), LIU Zhaowen(刘朝文), ZHANG Jianwen(张建文) and CHEN Jianfeng(陈建峰)****

Key Lab for Nanomaterials, Ministry of Education; research center of the ministry of education for high gravity engineering and technology, Beijing university of chemical technology, beijing 100029, China

**Abstract** A thermodynamic model has been developed to determine the reaction conditions favoring low temperature direct synthesis of barium titanate ($BaTiO_3$). The method utilizes standard-state thermodynamic data for solid and aqueous species and a Debye-Hückel coefficients model to represent solution nonideality. The method has been used to generate phase stability diagrams that indicate the ranges of pH and reagent concentrations, for which various species predominate in the system at a given temperature. Also, yield diagrams have been constructed that indicate the concentration, pH and temperature conditions for which different yields of crystalline $BaTiO_3$ can be obtained. The stability and yield diagrams have been used to predict the optimum synthesis conditions (*e.g.*, reagent concentrations, pH and temperature). Subsequently, these predictions have been experimentally verified. As a result, phase-pure perovskite $BaTiO_3$ has been obtained at temperature ranging from 55 to 85℃ using $BaCl_2$, $TiCl_4$ as a source for Ba and Ti, and NaOH as a precipitator.

**Keywords** nanoparticles synthesis, thermodynamic modelling, barium titanate, perovskite phase

## 1 INTRODUCTION

Barium titanate ($BaTiO_3$), a perovskite structure, has been widely investigated because of its dielectric and ferroelectric properties[1,2]. Recent years have witnessed significant advances in the chemical synthesis of perovskites for a variety of applications, using techniques such as hydrothermal synthesis[3], coprecipitation[4], and sol-gel synthesis[5]. These techniques involve chemical reactions among precursor materials in an aqueous environment. More recently, a low temperature direct synthesis (LTDS) technique[6–8] has received considerable attention from the scientific and engineering communities. The success of these methods to produce the desired material with specific characteristics depends to a large extent on process parameters, such as pH, composition and temperature. In order for LTDS to be commercialized, engineering approaches must be available to facilitate rapid technology development. However, a majority of the investigations that has been done in the past has used Edisonian trial and error methods for process development. This type of experimental approach suffers from its time-consuming nature and the inability to clearly discern between processes that are controlled by either thermodynamics or kinetics.

Recently, Lencka and Riman[9–11] proposed a thermodynamic model of heterogeneous system that makes it possible to predict the equilibrium states of hydrothermal reactions from $Ba(OH)_2$ solution and $TiO_2$ solid phase and indicate the range of reaction conditions that facilitate formation of the desired $BaTiO_3$ phase. This model was shown to be very useful for engineering and optimizing the hydrothermal synthesis of perovskites. The calculated stability diagrams have also shown that quantitative formation of $BaTiO_3$ is possible even at temperatures < 100℃. Therefore, considering the hydrothermal synthesis of $BaTiO_3$ particles using the thermodynamic model of Lencka and Riman, it is possible to obtain $BaTiO_3$ particles through common chemical precipitation methods at lower temperatures and pressures. However, they did not conclude further. Typically, low temperature aqueous synthesis at ambient pressure is preferred over hydrothermal synthesis in preparation of perovskites due to ease of reaction control, operation and scalability to commercial production capacity.

In this study, we seek to adapt a thermodynamic model for hydrothermal synthesis to predict the range of LTDS conditions for $BaTiO_3$ thermodynamic stability and perform the reactions experimentally to verify the predictions. In choosing the best synthesis conditions, we emphasize on using simple feedstock without having to pre-treat them and on minimizing the reaction temperature. Also, we focus on avoiding contamination of $BaTiO_3$ with any undesirable byprod-

Received 2004-11-02, accepted 2005-01-21.

* Supported by the National Natural Science Foundation of China (No. 20236020, No. 20325621), 863 Hi-Technology Research and Development Program of China (No. 2001AA325014), the Talent Training Program of the Beijing City (No. 9558103500), and the Fok Ying Tung Foundation (No. 81063).

** To whom correspondence should be addressed. E-mail: chenjf@mail.buct.edu.cn

ucts (*e.g.*, $BaCO_3$ or $TiO_2$) so that a pure crystalline powder can be obtained in single step.

## 2 THERMODYNAMIC MODEL

The thermodynamic model[9] provides a tool for calculating equilibrium concentrations of each species in a system as a function of temperature, pressure, pH, and the initial amount of reactants. The model is formulated for $k$ independent reactions. The $j$-th reaction ($j = 1, \cdots, k$) can be written as

$$\sum_{i=1}^{n_j} \nu_i^{(j)} A_i^{(j)} = 0 \quad j = 1, \cdots, k \tag{1}$$

where $A_i^{(j)}$ is the $i$-th chemical species participating in the $j$-th reaction, $\nu_i^{(j)}$ is the stoichiometric number of species $A_i^{(j)}$ and $n_j$ is the total number of species undergoing the $j$-th reaction.

The equilibrium state of the $j$-th reaction is defined by the standard Gibbs energy change of the reaction

$$\Delta G^0_{\mathrm{RXN},j} = \sum_{i=1}^{n_j} \nu_i^{(j)} G^0_{\mathrm{f}}(A_i^{(j)}) = -RT \ln K_j(T,p) \quad j = 1, \cdots, k \tag{2}$$

where $G^0_f(A_i^{(j)})$ is standard Gibbs energy of formation of species $A_i^{(j)}$ and $K_j$ is the equilibrium constant of the $j$-th reaction. Since molality $m$ is used in this work as the concentration unit, the equilibrium constant is expressed as

$$K_j(T,p) = \prod_{i=1}^{n_j} (m_{A_i^{(j)}} \gamma_{A_i^{(j)}})^{\nu_i^{(j)}} \quad j = 1, \cdots, k \tag{3}$$

where $\gamma_{A_i^{(j)}}$ is the activity coefficient of species $A_i^{(j)}$.

The chemical equilibrium Eqs. (2) and (3) are solved simultaneously with mass and electroneutrality balance equation. To solve this system of equations, the standard Gibbs energies of formation and activity coefficients should be known.

To construct the thermodynamic model, the value of the standard Gibbs energies of formation ($\Delta G^0_{\mathrm{f}}$) for all the species considered in the system are required. For accuracy of information on the stability of various phases in a system, as many species as possible need to be considered, restricted only by the availability of the thermodynamic data. In addition, it is desirable to obtain the values of $\Delta G^0_{\mathrm{f}}$ as a function of temperature, to facilitate the construction of the equilibrium diagrams at various temperatures. The standard Gibbs energy of formation for each species can be calculated as a function of temperature, if the values of the heat of formation ($\Delta H^0_{\mathrm{f}}$), and entropy ($S^0$) at a reference temperature (usually 25℃) as well as the heat capacity ($C_p^0$) as a function of temperature ($T$) are known. From this set of values, the $\Delta G^0_f$ can be calculated using standard thermodynamic relations[12].

Thermodynamic data for several species in the Ba-Ti-C system have been compiled by Lencka and coworkers[9—11]. For many species, the data are readily available in several existing compilations of thermochemical data[13—15]. For species that are not available in the existing databases, Lenka and Riman have used a computer program[16] that uses the Helgeson-Kirkham-Flowers (HKF) estimation method to predict the standard thermodynamic data. Moreover, they have critically evaluated the consistency of these data by verifying the conformity of the relations between the experimental values to the general relations of thermodynamics. The data for additional, usually minor, species that are not considered by Lenka and Riman are obtained from existing thermodynamic databases as well as the database included in HSC Chemistry for Windows[17], the computer program used to calculate and plot the phase stability diagrams in the current work. However, thermodynamic data for some species, such as $TiCl^{3+}$, $TiCl_2^{2+}$, $TiCl_3^{+}$, and their hydrolyzed species, are not available and therefore are not considered in the calculation of the diagrams. Table 1 lists the values of $\Delta G^0_f$ at 25, 55, and 85℃ for the species that may exist in significant quantities in the Ba-Ti LTDS system. Since atmospheric carbon dioxide can play a role in the synthesis, data for $CO_2$-derived species are also given in Table 1.

The activity coefficient model has been described in the previous work[9]. Therefore, only the main relations will be summarized here. The model, developed by OLI Systems, Inc.[18], is based on a combination of models published by Bromley[19] and Pitzer[20]. The activity coefficient of an ion $i$ is expressed as

$$\lg\gamma_i = DH_i + BZ_i + P_i \tag{4}$$

where $DH_i$ is the Debye-Hückel term representing long-range electrostatic interactions, $BZ_i$ is the Bromley-Zemaitis term for short-range ion-ion interactions, and $P_i$ is the Pitzer term for ion-neutral molecule interactions.

The Debye-Hückel term is given by

$$DH_i = \frac{-A|Z_i|^2 I^{1/2}}{1 + I^{1/2}} \tag{5}$$

$$I = 0.5 \sum_i Z_i^2 m_i \tag{6}$$

where $A$ is the Debye-Hückel coefficient that depends on temperature and solvent properties, $Z_i$ is the number of charges on ion $i$, $I$ is the ionic strength, and $m_i$ is the molality of species $i$.

**Table 1 Free Gibbs energy of formation data for Ba-Ti-C species at 298.15, 328.15 and 358.15 K and $1.01\times10^5$ Pa pressure**

| Species | $\Delta G_f^0$, kJ·mol$^{-1}$ | | | Ref. |
|---|---|---|---|---|
| | 298.15K | 328.15K | 358.15K | |
| $H^+$ | 0 | 0 | 0 | |
| $BaOH^+$ | −716.72 | −713.40 | −710.06 | 9, 21 |
| $BaHCO_3^+$ | −1153.5 | −1148.0 | −1142.0 | 9, 16 |
| $Ba^{2+}$ | −560.78 | −563.12 | −565.20 | 9, 16 |
| $Ti^{4+}$ | −354.18 | −339.78 | −323.97 | 9, 21 |
| $TiOH^{3+}$ | −614.00 | −607.78 | −600.67 | 9, 21 |
| $Ti(OH)_2^{2+}$ | −869.56 | −868.00 | −865.70 | 9, 21 |
| $Ti(OH)_3^+$ | −1092.5 | −1094.0 | −1095.2 | 9, 21 |
| $OH^-$ | −157.3 | −150.06 | −142.98 | 9, 22 |
| $CO_3^{2-}$ | −527.98 | −512.57 | −496.23 | 9, 16 |
| $HCO_3^-$ | −586.94 | −576.38 | −565.74 | 9, 16 |
| $HTiO_3^-$ | −955.88 | −959.58 | −963.63 | 9, 22 |
| $H_2O$ | −237.25 | −232.47 | −227.90 | 9, 22 |
| $Ti(OH)_4$ | −1318.3 | −1298.8 | −1279.5 | 9, 21 |
| $CO_2$ | −385.97 | −383.68 | −382.35 | 9, 16 |
| $BaCO_3(aq)$ | −1103.9 | −1094.5 | −1084.9 | 16, 22 |
| $Ba(OH)_2$ | −855.2 | −846.4 | −837.8 | 9, 21 |
| $BaCO_3$ | −1164.8 | −1158.1 | −1150.2 | 9, 16 |
| $BaTiO_3$ | −1572.4 | −1563.7 | −1555.1 | 9, 15 |
| $BaO$ | −525.35 | −522.64 | −519.90 | 9, 15 |
| $Ba(OH)_2{\cdot}8H_2O$ | −2779.9 | −2723.4 | −2666.3 | 9, 21 |
| $Ba_2TiO_4$ | −2132.9 | −2121.8 | −2110.8 | 9, 15 |
| $TiO_2$ | −890.70 | −885.10 | −879.54 | 9, 16 |

The Bromley-Zemaitis term is expressed as

$$BZ_i=\sum_{j=1}^{NO}\left[\frac{|Z_i|+|Z_j|}{2}\right]^2\beta_{ij}m_j \tag{7}$$

$$\beta_{ij}=\frac{(0.06+0.6B_{ij})|Z_iZ_j|}{(1+1.5I/|Z_iZ_j|)^2}+B_{ij}+C_{ij}I+D_{ij}I^2 \tag{8}$$

where $NO$ is the number of ions with charge opposite to that of the ion $i$, and $B_{ij}$, $C_{ij}$, and $D_{ij}$ are temperature-dependent parameters for cation-anion interactions.

The Pitzer term $P_i$ is given by

$$P_i=\sum_{j=1}^{NM}BP_{ij}m_j+\frac{Z_i^2}{4I^2}BPS_j \tag{9}$$

$$BP_{ij}=\beta_{ij}^{(0)}+\beta_{ij}^{(1)}+(1+2I^{1/2})[1-\exp(-2I^{1/2})]/2I \tag{10}$$

$$BPS_j=0.86859m_j\sum_{k=1}^{NS}BPP_{jk}m_k \tag{11}$$

$$BPP_{jk}=\beta_{jk}^{(1)}[1-(1+2I^{1/2}+2I)\exp(-2I^{1/2})] \tag{12}$$

where $NM$ is the number of molecular species, $NS$ is the total number of species in solution, and $\beta_{ij}^{(0)}$ and $\beta_{ij}^{(1)}$ are temperature-dependent parameters for each ion-molecule and molecule-molecule pair.

The activity coefficients of nonionic species other than water include only the Pitzer term

$$\lg\gamma_i=2\sum_{j=1}^{NS}BP_{ij}m_i \tag{13}$$

The activity of water is obtained by applying the Gibbs-Duhem equation to the above expressions.

The expressions for activity coefficients [Eqs. (4) to (13)] are inserted into chemical equilibrium equation [Eqs. (2) and (3)]. Subsequently, the combined set of chemical equilibrium expressions and material and electroneutrality balances are solved using the OLI Systems software[18] or by our own model.

## 3 THEORETICAL PREDICTION

The thermodynamic model is used to generate stability diagrams that show which species predominate in the system at a fixed temperature and pressure. In all cases, ambient pressure was assumed. As independent variables, we use the pH of the solution and the total molality of a selected component. The total molality ($m_{\mathrm{Me,T}}$, in units of moles of solute per 1 kg of water) refers to the equilibrium concentration of dissolved metal species containing the metal Me, and does not include those compounds that precipitate from the solution. Two kinds of boundaries are shown in the diagrams: those between two aqueous species and those between a solid and an aqueous species. The boundaries between two aqueous species denote the loci where both species have equal concentrations whereas those between solid and aqueous species correspond to the beginning of precipitation of the solid. In practice, an equilibrium point was assumed to lie on the solid-aqueous species boundary when less than 0.25% of the feedstock was found to be in the form of a solid phase, which was consistent with the hydrothermal model of Lencka and Riman[9].

Figure 1 shows the stability diagrams calculated at 298.15 K using ideal solution approximation (*i.e.*, with all activity coefficients assumed to be equal to 1). Note that the effect of $CO_2$ has been neglected. Lencka and Riman independently processed the data of Barin[13] and Naumov[14] using the hydrothermal model to yield the results, also shown in Fig. 1. It is obvious that Fig. 1 could illustrate the effect of using data based on different standard states on the phase stability diagram. At the same time, it also compares the model in this study with the hydrothermal model of Lencka and Riman.

As shown in Fig. 1, the difference between standard data can shift the boundaries between phase stability regions by as much as 1—1.5 pH units. While the Naumov *et al.*[14] compilation provides data recommended on the basis of literature comparisons, their consistency does not appear to have been checked. Thus, in this study, following the works of Lencka and Riman on their hydrothermal model, the data of Barin[13] was mostly adopted. When selecting similar data values and treating solutions as ideal solutions, the model outcome is not affected regardless of hydrothermal synthesis or LTDS when the temperature is at 298.15 K. This is demonstrated in Fig. 1. Agreement of our model computed results with the hydrothermal model of Lencka and Riman at the temperature of 298.15 K suggests that the model calculation is correct.

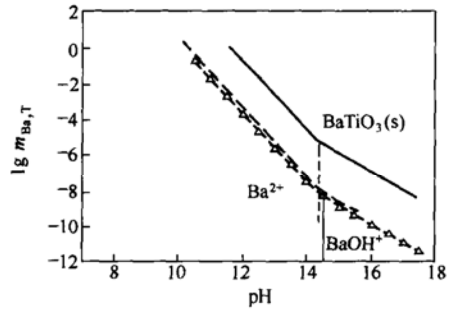


**Figure 1 Calculated stability for the Ba-Ti system using an ideal-solution approximation at 298.15 K**
The solid and dashed lines denote the hydrothermal model results obtained using the data of Barin and Naumov *et al.* by ProChem Software[18], respectively
- -△- - ideal-solution model result

Figure 2 shows the results obtained from the thermodynamic model with and without ideal solution approximation. For simplicity, the effect of $CO_2$ is neglected and the calculation of solution non-ideality is based on Debye-Hückel coefficient. For comparison, the calculated results of the hydrothermal model of Lencka and Riman, based on ideal solution and non-ideal solution, are also shown in Fig. 2. Note that Lencka and Riman employed Eq. (4) as activity coefficients for non-ideal solutions. In these cases, the boundaries are shown between aqueous $Ba^{2+}$ and solid $BaTiO_3$(s), aqueous $Ba^{2+}$ and $BaOH^+$, and aqeous $BaOH^+$ and solid $BaTiO_3$(s). As evident from Fig. 2, the phase boundaries calculated from the modeled activity coefficients and simplified (ideal solution) models are markedly different. In contrast to the ideal-solution case, the phase boundaries calculated from the activity coefficients model are no longer represented by straight lines. Their curvature is especially significant for higher concentrations of aqueous species ($m_{Ba,T} > 10^{-3}$). This is attributed to the influence of solution non-ideality on the location of the boundary. Thus, it indicates that solution non-ideality can shift the phase boundaries towards higher pH values. At the same time, an implication is that, in order to obtain barium titanate crystalline particles from real solutions, a higher pH than that of ideal solution calculation is required. There is no significant difference between using the Debye-Hückel model for the activity coefficients and the Lencka and Riman model. Thus, to simplify subsequent calculations, this study only employs the Debye-Hückel model to obtain activity coefficients for solution non-ideality.

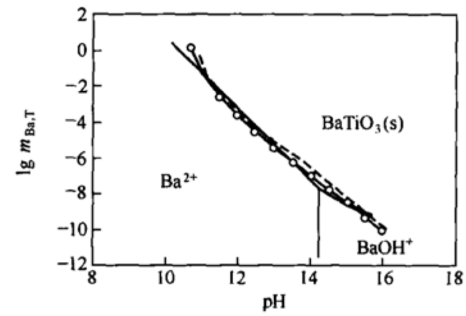


**Figure 2 Calculated stability diagram for the Ba-Ti system at 298.15 K with and without using modeled activity coefficients**
Standard state data were taken from the compilation of Barin[15]. For comparison, the hydrothermal modeled results employing Eq. (4) as activity coefficients for non-ideal solutions by ProChem Software[18] are also shown as dashed line
- - ○ - - Using modeled activity coefficients;
—— using ideal-solution approximation

Phase stability diagrams demonstrate the effect of process variables, such as $m_{Ba,T}$, pH, $T$ and Ba/Ti ratio, on the formation of $BaTiO_3$ (s). Barium titanate particles can be obtained in the whole range of $m_{Ba,T}$ provided that pH is appropriately chosen. It is obvious that high temperature and pH value favors formation of barium titanate crystals if the $m_{Ba,T}$ was chosen. When the pH value and temperature are given, the barium and titanium ionic concentrations in the feed are crucial. From Fig. 3, it can be seen that phase stability diagram is temperature-dependent. As the temperature rises, the boundary moves towards lower

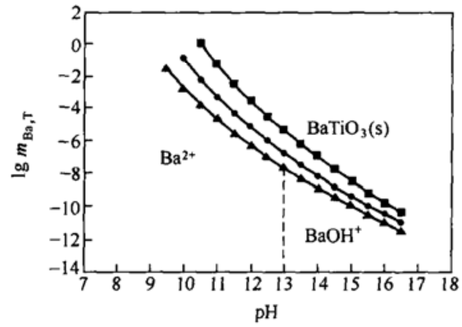


**Figure 3 Calculated stability diagram for the Ba-Ti system at 298.15, 328.15 and 358.15 K using Debye-Hückel equation as modeled activity coefficients**
Standard state data were taken from the compilation of Barin[15]
$T$, K: —■— 298.15; —●— 328.15; —▲— 358.15

pH values. This implies that a high temperature is necessary for preparation of barium titanate particles and may require a lower precipitator (*i.e.* NaOH) concentration.

The formation of $BaTiO_3$ (s) consumes equimolar amounts of Ba and Ti. If different relative amounts of Ba and Ti are used (Ba/Ti≠1), the location of the phase boundary does not change. However, this affects the final solid mixture composition and quantities. For instance, according to the model results, excess Ti(Ba/Ti<1) would cause acontamination of $BaTiO_3$ with $TiO_2$ (s), which is stable under low temperature aqueous synthesis. This proves that Ba/Ti ratio should not be less than 1 to avoid $TiO_2$(s) contamination. When barium is in excess, the model showed that at high pH (pH>15), $Ba(OH)_2{\cdot}8H_2O$ side-product forms, which, if in excess, requires several washing for removal. Thus, it is necessary to avoid too much $Ba^{2+}$ during preparation of barium titanate.

The proposed generalized thermodynamic model makes it possible to analyze the effect of $CO_2$(g) on the low temperature direct synthesis of barium titanate particles. Carbon dioxide acts as a contaminant due to its appreciable concentration in the atmosphere. In the abovementioned Ba-Ti system model, species with relation to $CO_2$ can be added, such as in the form of $BaCO_3$(s), $BaCO_3$ (aq), $CO_2$ (aq), $BaHCO_3^+$, $HCO_3^+$, $CO_3^{2+}$, to enable calculation of the Ba-Ti-C system model (Fig. 4). From Fig. 4, it can be seen that in an open system with respect to $CO_2$ (g), desirable $BaTiO_3$(s) can not form under any temperature and pH conditions, as $BaCO_3$(s) is inherently more stable than $BaTiO_3$(s). $BaCO_3$(s) precipitates at lower pH values than those needed to precipitate $BaTiO_3$(s). Therefore, this suggests that the exposure to $CO_2$ should always be avoided while synthesizing $BaTiO_3$(s).

The stability diagrams indicate the ranges of thermodynamic variables for which the desired product is stable. However, they do not give any information about the yield of $BaTiO_3$ in relation to the precursor materials. This information is provided by yield diagrams, which show the yield of barium titanate as a function of pH and the input concentration of barium. It should be noted that the input concentration of Ba ($m_{\mathrm{Me,In}}$) differs from the total concentration of barium in solution ($m_{\mathrm{Me,T}}$) in that it encompasses all barium-containing solution species and barium titanate crystals for Ba/Ti=1 or all barium-containing solution species and all solid phases which are stable at Ba/Ti>1. The yield diagrams show the pH and $m_{\mathrm{Me,In}}$ ranges for which the yield is higher than 99.99%, and those for which the yield is less than 99.99%. The yield diagrams have been constructed for the stoichiometric mole ratio Ba/Ti=1.0. Therefore, an incomplete yield indicates that the obtained $BaTiO_3$ is contaminated with solid $TiO_2$.

Figure 5 shows the yield diagram for low temperature direct synthesis of barium titanate particles at 298.15 K, 328.15 K and 358.15 K. Since very low feed concentrations (*e.g.* less than $10^{-6}$ mol·kg$^{-1}$) have no significance in practical synthesis, the figure only provides the production yield diagram for feed concen

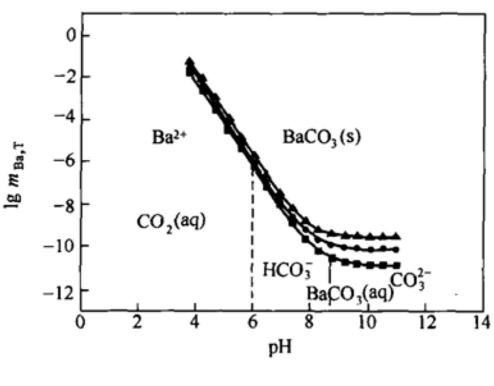


**Figure 4 Calculated stability diagram for the Ba-Ti system under air corresponding to a fixed partial pressure of $CO_2$ (g) ($p_{CO_2(g)}$ = 33.54 Pa) at 298.15, 328.15 and 358.15 K**
*T*, K: —■— 298.15; —●— 328.15; —▲— 358.15

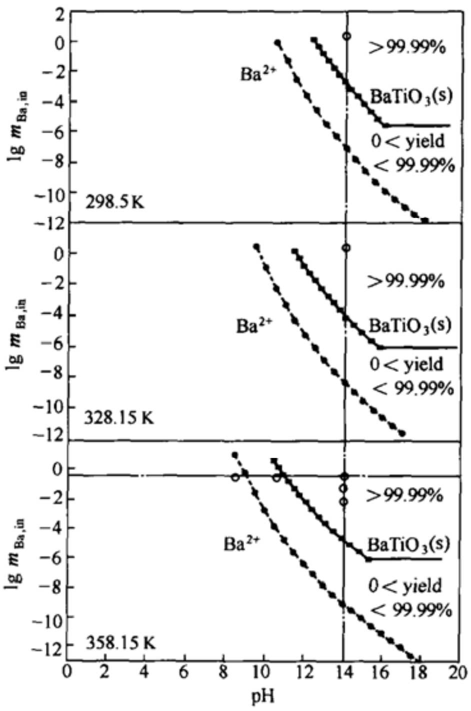


**Figure 5 Calculated yield diagram for the low temperature aqueous synthesis of $BaTiO_3$ at 298.15 K, 328.15 K and 358.15 K from $BaCl_2$ and $TiCl_4$ as precursors and NaOH as precipitator**
Symbols (●) denote the conditions of experimental synthesis performed
—■— yield curve; - - ● - - phase stability curve

tration of $10^{-6}$ mol·kg$^{-1}$ and above. In addition, the marked locations in the diagram represent the data-points in this study to be verified experimentally under controlled conditions. From Fig. 5, the phase stability diagrams provide information about the conditions of incipient precipitation of various solid phases. Between the boundary of stability diagram and the yield curve, barium titanate and titanium dioxide co-exist. Pure barium titanate crystals are obtained only beyond the yield curve. The figure also indicates that, to obtain pure barium titanate crystalline particles, the higher pH value than phase stability curve should be sustained for reaction (for example, at a temperature of 328.15 K, the pH needs to be at least 12.0). Furthermore, the lower the reaction temperature, the higher the required pH condition. In this study, it implies that a significantly high initial NaOH concentration should be required, since precipitation of 1 mol barium titanate will consume 6 mol NaOH according the reaction equation. Thus, based on economical and environmental considerations and results from the thermodynamic model, the reaction temperature should be as high as 328.15 K.

## 4 EXPERIMENTAL PROCEDURE

All reagents of chemical grade (*i.e.* $BaCl_2 \cdot H_2O$, $TiCl_4$, NaOH) were used without further purification. All solutions were filtered through 0.45 $\mu$m pore size membranes to remove the particulate impurities before use. A certain amount of $TiCl_4$ solution was added to the solution of $BaCl_2$ with constant rate of stirring at room temperature until fully mixed. The mixed $BaCl_2$-$TiCl_4$ solution was filtered to remove the particulate impurities. A 1.0 L glass reaction vessel fitted with a condenser, thermocouple, gas inlet, and sampling dip tube was used. In a "standard" run, 300 ml mixed chlorides solution was instantaneously added into the reactor, which was previously filled with some NaOH solution, at a constant flow rate under stirring. The temperature of reactor was controlled by means of a thermostatic bath. The concentration of reactants varied between 0.01 mol·kg$^{-1}$ and 0.5 mol·kg$^{-1}$. The temperature was varied of 298.15 K to 358.15 K. Syntheses were performed with a stoichiometric ratio Ba/Ti=0.95, 1.07 and 1.2 for a wide range of pH. The pH of the solution was maintained at the correct level using NaOH as precipitator. The necessary amount of the precipitator was obtained from the calculations.

Phase identification was conducted using an X-ray diffractometer (Shimadzu XRD-6000, Japan) with Cu K$\alpha$ radiation at a scan speed of 4°/min. Particle size and morphology of selected as-prepared powders was characterized *via* TEM (Model Hitachi H-800, Cambridge, UK) using bright-field analysis at an accelerating voltage of 120 kV. This instrument was equipped with a system with the potential of performing selected area electron diffraction (SAED) to further characterize particle structures.

## 5 SYNTHESIS RESULTS

To verify the thermodynamic modeling, the synthesis of $BaTiO_3$ was performed for several points on the yield diagrams. Table 2 shows the characterization results of as-synthesized powder at different reaction conditions.

When the reaction temperature is at 298.15 K, regardless of the concentration and pH conditions, the experiment results indicated that the prepared particles are of predominately irregular amorphous phase. Furthermore, there are also small amounts of barium carbonate and NaCl (No. 1 of Table 2.). Even if the reaction time has been extended to 1 hour, it still could not synthesize barium titanate crystals. At these experimental points, the results were not in agreement with predictions. The difference between predictions

**Table 2 Experimental conditions and results for the preparation of $BaTiO_3$ by the LTDS process**

| No. | Temp., ℃ | pH | $[BaCl_2]_{stock}$, mol·kg$^{-1}$ | Ratio$_{stock}$ $BaCl_2/[TiCl_4]$ | Primary phase | Minor phase | Morphology |
|---|---|---|---|---|---|---|---|
| 1 | 25 | 14 | 0.5 | 1.07 | AM | BC, NA | I, A |
| 2 | 55 | 14 | 0.5 | 1.07 | BT | BC, AM | S, A |
| 3 | 85 | 14 | 0.5 | 1.07 | BT | | S |
| 4 | 85 | 14 | 0.5 | 0.95 | BT | AM | S, I, A |
| 5 | 85 | 14 | 0.5 | 1.2 | BT | BC | S |
| 6 | 85 | 14 | 0.1 | 1.07 | AM, BC | BT | I, A, S |
| 7 | 85 | 14 | 0.01 | 1.07 | AM | BC | I, A |
| 8 | 85 | 9 | 0.5 | 1.07 | AM | BC, NA | A, I |
| 9 | 85 | 12 | 0.5 | 1.07 | BT | AM, BC | S, A |

Standard conditions, reaction time 10 min

AM: amorphous phase; BC: $BaCO_3$ (Witherite, JCPDS No. 05-0378); BT: cubic $BaTiO_3$ (JCPDS No. 31-0174); NA: NaCl (Halite, JCPDS No. 05-0628).

S: spheres; A: aggregates; I: irregular.

and experimental results may have been due to sluggish reaction kinetics at low temperature. As in the case of any thermodynamic calculation, phase and yield diagrams are constructed with an assumption of thermodynamic equilibrium between the species and indicate regions of thermodynamic stability and boundaries of thermodynamic equilibria. However, these diagrams do not provide any information regarding the kinetics of reactions. When the temperature is at 328.15 K, the experimental results (No. 2 of Table 2) show that the particles are predominantly cubic-phase barium titanate, and amorphous titanium dioxide also exist as second phase. This discrepancy between experiment and thermodynamic model prediction could also be due to sluggish reaction kinetics. Subsequent extension of reaction time resulted in the removal of amorphous titanium dioxide and increase of barium carbonate content in the particles. The reason is the prolonged contact of atmospheric carbon dioxide with the reaction system. This observation confirms the validity of the thermodynamic model since the model results also imply that the reaction system should avoid contact with carbon dioxide during LTDS method of barium titanate synthesis. For the reaction at temperature of 358.15 K, the result of experimental points under high $Ba^{2+}$ ionic concentration was consistent with the model counterpart (for example, pure barium titanate particles are obtained at pH 14.0. Then, when pH value is at 12.0, the particles become a mixture of cubic phase barium titanate and amorphous titanium dioxide. Finally, when pH value is at 9.0, amorphous titanium dioxide predominates, with small amounts of barium carbonate present. See No. 3, 8 and 9 of Table 2.). However, a discrepancy exists when $Ba^{2+}$ concentration is low. For example, the experiment result indicated that although the pH value is as high as 14 and the reaction temperature is of 358.15 K, the crystalline particle phase contains a certain amount of amorphous titanium dioxide under conditions of $Ba^{2+}$ concentration of $0.1\,mol\cdot kg^{-1}$, and when the $Ba^{2+}$ concentration is $0.01\,mol\cdot kg^{-1}$, the XRD pattern of the particle phase did not contain the signature peaks of barium titanate (No. 6, 7 of Table 2.). The difference between predictions and experimental results indicates that the phase transformation from precursor to perovskite is not complete at reaction time of 10 min at low $Ba^{2+}$ concentration even with high temperature because of sluggish reaction kinetics.

It is obviously that the condition of high temperature and high $Ba^{2+}$ concentration promotes the reaction kinetics and is more favorable for the preparation of phase-pure perovskite $BaTiO_3$. Using the results of the thermodynamics model at conditions of 358.15 K, pH 14 and $Ba^{2+}$ concentration of $0.5\,mol\cdot kg^{-1}$, we successfully prepared nano-sized particles of barium titanate (No. 3 of Table 2 and Fig. 6). The results of this study indicate that theoretical predictions of synthesis condition using the thermodynamic modeling can be reconciled to the experimental results except in the low temperature region (*i.e.*, $< 328.15$ K) and at low $Ba^{2+}$ concentration (*i.e.* $< 0.1\,mol\cdot kg^{-1}$) and it is possible to predict the synthesis conditions of phase-pure $BaTiO_3$ powder in the Ba-Ti-$H_2O$ system.

Process variables, such as temperature, pH, reactant concentration, are thermodynamic variables but they also influence both reaction and crystallization kinetics. However, it should be realized that non-thermodynamic variables associated with reactors used to crystallize the ceramic powders are also important when operating in thermodynamically controlled processing variable space. Using Fig. 6 to define the phase space, decreasing the stirring speed from 450 to $5.0\,r\cdot min^{-1}$ can change the particle size and particle size distribution. This is a very important capability of LTDS, since it allows inputting specific particle size, particle size distribution, and morphology for a process and changing it to suit the requirements of the user. Furthermore, it simplifies the process greatly since all other reaction conditions are held constant. A further study of kinetics and particle formation mechanism of nanometer $BaTiO_3$(s) will be conducted and discussed separately[23].

## 6 CONCLUSIONS

Electrolyte thermodynamics makes it possible to determine the optimum conditions ($T$, pH, concentrations, Ba/Ti ratio) for the synthesis of crystalline $BaTiO_3$ from simple precursors such as $BaCl_2\cdot 2H_2O$ and $TiCl_4$. Also, it clarified the conditions that are undesirable for the synthesis because the barium titanate is either unstable or contaminated with other solids. As convenient predictive tools, stability and yield diagrams were constructed for various temperatures. These diagrams subsequently were used to design practical syntheses in order to verify the result of theoretical predictions. Experimental syntheses were performed in the whole temperature range using $BaCl_2$ and $TiCl_4$ for the whole range of pH and for stoichiometric and nonstoichiometric Ba/Ti ratios.

Both theory and experiment indicated that the formation of $BaTiO_3$ strongly depends on pH and less so on the concentration of Me ($m_{Me,T}$) species. In addition, carbon dioxide exposure should be avoided since it leads to the precipitation of a $BaCO_3$(s) impurity phase. However, in the lower temperature range ($T < 328.15$ K) and at lower $Ba^{2+}$ concentration ($m_{Ba} < 0.1\,mol\cdot kg^{-1}$), although the thermodynamic model predicted, pure crystalline $BaTiO_3$ cannot be obtained by direct precipitation from solution. Thus, our predictions are not corroborated by experimental results. This discrepancy may be due to sluggish reaction kinetics at lower temperatures or low concentration of initial $Ba^{2+}$ as well as the limited availability of thermochemical data for some species.

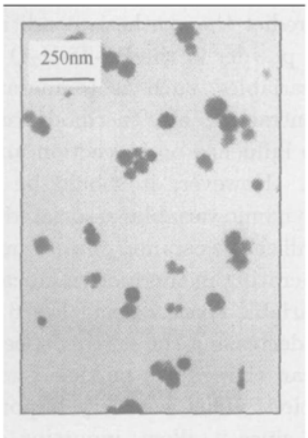


(a) Stirring speed is $450\,r{\cdot}min^{-1}$


(b) Stirring speed is $5\,r{\cdot}min^{-1}$

**Figure 6 $BaTiO_3$ powders prepared by low temperature direct synthesis at 85℃ for 10 min**

In both cases $BaCl_2$ and $TiCl_4$, were used as sources of Ba and Ti. Total concentration of (Ba+Ti) was $1.0\,mol{\cdot}kg^{-1}$, concentration of the NaOH precipitator was $6\,mol{\cdot}kg^{-1}$, and the Ba/Ti ratio was 1.07


## ACKNOWLEDGMENTS

*We would like to thank Mr. Wang L.-S of OLI Systems Inc. for providing the thermodynamic modeled calculation of hydrothermal synthesis.*


## NOMENCLATURE

| | |
|---|---|
| $A$ | the Debye-Hückel coefficient that depends on temperature and solvent properties |
| $A_i^{(j)}$ | the $i$-th chemical species participating in the $j$-th reaction |
| $B_{ij}$ | temperature-dependent parameters for cation-anion interactions |
| $BZ_i$ | the Bromley-Zemaitis term for short-range ion-ion interactions |
| $C_{ij}$ | temperature-dependent parameters for cation-anion interactions |
| $C_p^0$ | the standard heat capacity, $J{\cdot}mol{\cdot}K^{-1}$ |
| $DH_i$ | the Debye-Hückel term representing long-range electrostatic interactions |
| $D_{ij}$ | temperature-dependent parameters for cation-anion interactions |
| $G_f^0(A_i^{(j)})$ | the standard Gibbs energy of formation of species $A_i^{(j)}$, $kJ{\cdot}mol^{-1}$ |
| $\Delta G_f^0$ | the standard Gibbs energies of formation, $kJ{\cdot}mol^{-1}$ |
| $\Delta G_{RXN,j}^0$ | the standard Gibbs energy change of the reaction $j$, $kJ{\cdot}mol^{-1}$ |
| $\Delta H_f^0$ | the standard heat of formation, $kJ{\cdot}mol^{-1}$ |
| $I$ | the ionic strength |
| $K_j$ | the equilibrium constant of the $j$-th reaction |
| $m_i$ | the molality of species $i$ |
| $m_{Ba,T}$ | The total molality of $Ba^{2+}$, $mol{\cdot}kg^{-1}$ |
| $m_{Me,T}$ | the total molality, $mol{\cdot}kg^{-1}$ |
| $n_j$ | the total number of species undergoing the $j$-th reaction |
| $NM$ | the number of molecular species |
| $NO$ | the number of ions with charge opposite to that of the ion $i$ |
| $NS$ | the total number of species in solution |
| $R$ | universal gas constant, $J{\cdot}mol^{-1}{\cdot}K^{-1}$ |
| $P_i$ | the Pitzer term for ion-neutral molecule interactions |
| $p$ | pressure, Pa |
| $S^0$ | the standard entropy, $J{\cdot}mol^{-1}{\cdot}K^{-1}$ |
| $T$ | temperature, K |
| $Z_i$ | the number of charges on ion $i$ |
| $\beta_{ij}^{(0)}$ | temperature-dependent parameters for each ion-molecule pair |
| $\beta_{ij}^{(1)}$ | temperature-dependent parameters for each molecule-molecule pair |
| $\nu_i^{(i)}$ | the stoichiometric number of species $A_i^{(j)}$ |
| $\gamma_{A_i^{(j)}}$ | the activity coefficient of species $A_i^{(j)}$ |

## REFERENCES


1 Chandler, C.D., Roger, C., Hampden-Smith, M.J., "Chemical aspects of solution routes to perovskite-phase mixed-metal oxides from metal-organic precursors", *Chem. Rev.*, **93**, 1205—1241 (1993).

2 Pena, M.A., Fierro, J.L.G., "Chemical structures and performance of perovskite oxides", *Chem. Rev.*, **101**, 1981—2017 (2001).

3 Oledzka, M., Brese, N.E., Riman, R.E., "Hydrothermal synthesis of $BaTiO_3$ on a titanium loaded polymer support", *Chem. Mater.*, **11** (7), 1931—1935 (1999).

4 Ver der Gijp, S., Emond, M.H.J., "Preparation of $BaTiO_3$ by homogeneous precipitation", *J. Eur. Ceram. Soc.*, **19** (9), 1683—1690 (1999).

5 Viswanasth, R.N., Ramasamy, S., "Preparation and ferroelectric phase transition studies of nanocrystalline $BaTiO_3$", *NanoStruct. Mater.*, **8** (2), 155—162 (1997).

6 Nanni, P., Leoni, M., Buscaglia, V., Aliprandi, G., "Low-temperature aqueous preparation of barium metatitanate powders", *J. Eur. Ceram. Soc.*, **14**, 85—90 (1994).

7 Her, Y.S., Matijevic, E., Chon, M.C., "Preparation of well-defined colloidal barium titanate crystals by the controlled double-jet precipitation" *J. Mater. Res.*, **10** (2), 3106—3114 (1995).
8 Wade, S., Tsurumi, T., Chikamori, H., Noma, T., Suzuki, T., "Preparation of nm-sized $BaTiO_3$ crystallites by a LTDS method using a highly concentrated aqueous solution" *J. Cryst. Growth*, **229**, 433—439 (2001).
9 Lencka, M.M., Riman, R.E., "Thermodynamic modeling of hydrothermal synthesis of ceramic powders", *Chem. Mater.*, **5**, 61—70 (1993).
10 Lencka, M.M., Riman, R.E., "Hydrothermal synthesis of perovskite materials: thermodynamic modeling and experimental verification", *Ferroelectrics*, **151**, 159—164 (1994).
11 Lencka, M.M., Riman, R.E., "Thermodynamics of the hydrothermal synthesis of calcium titanate with reference to other alkaline-earth titanates", *Chem. Mater.*, **7**, 18—25 (1995).
12 Barner, H.E., Scheuerman, R.V., Handbook of Thermochemical Data For Compounds and Aqueous Species, John Wiley & Sons, New York (1978).
13 Barin, I., Thermochemical Data of Pure Substances, VCH Publishers, Weinheim, Germany, (1989).
14 Naumov, G.B., Ryzhenko, B.N., Khodakovsky, I.L., Handbook of Thermodynamic Data, U. S. Geological Survey, Washington, DC (1974).
15 Barin, I., Thermochemical Data of Pure Substances, VCH Verlagsgesellschaft, Weinheim, Germany, (1993).
16 Johnson, J.W., Oelkers, E.H., Helgeson, H.C., SUPCRT92: A Software Package for Calculating the Standard Molal Thermodynamic Properties of Minerals, Gases, Aqueous Species, and Reactions From 1 to 5000 bar and 0—1000℃, University of California, Berkeley and Lawrence Livermore National Laboratory, Berkeley, CA (1991).
17 Roine, A., HSC Chemistry for Windows 2.03, Chemical Reaction and Equilibrium Software With Extensive Thermochemical Database, Outokumpu Research Oy, Pori, Finland (1994).
18 ProChem Software: Electrochem, V. 9.0, OLI Systems Inc. Morris Plains, NJ (1992).
19 Bromley, L.A., "Thermodynamic properties of strong electrolytes in aqueous solutions", *AIChE J.* **19**, 313—319 (1973).
20 Pitzer, K.S., "Thermodynamics of electrolytes. I. Theoretical basis and general equations", *J. Phys. Chem.*, **77**, 268—277 (1973).
21 Medvedev, V.A., Bergman, G.A., Gurvich, L.V., Yungman, V.S., Vorobiev, A.F., Kolesov, V.P., Thermicheskie Konstanty Veshchestv (Thermal constants of substances), Glushko, V.P., Ed., Vinitii, Moscow, Vol. 1—10, 1965—1982.
22 Venigalla, S., Adair, J.H., "Theoretical modeling and experimental verification of electrochemical equilibria in the Ba-Ti-C-$H_2O$ system", *Chem. Mater.*, **11**, 589—599 (1999).
23 Shen, Z.G., "Controlled Preparation and Characterization of Nano-$BaTiO_3$-Based Electro-Ceramic Powders", Ph. D. Thesis, Beijing University of Chemical Technology, Beijing, (2004).